第三十九届中国控制会议

The 39th Chinese Control Conference

程序册

Final Program

主办单位

中国自动化学会控制理论专业委员会

中国自动化学会

中国系统工程学会

承办单位

东北大学

Sponsoring Organizations

Technical Committee on Control Theory, Chinese Association of Automation

Chinese Association of Automation

Systems Engineering Society of China

Northeastern University, China

2020 年 7 月 27-29 日，中国 • 沈阳

July 27-29, 2020, Shenyang, China

Xiao, Jun — China Acad. of Engineering Physics
Zhu, Qidan — Harbin Engineering Univ.

▷ PTuB-75

0310 *The Determinants of Regional Credit Networks: Evidence from Chinese Guarantee System*

Wang, Yingli — Acad. of Mathematics & Sys. Sci., Chinese Acad. of Sci.
Lu, Chang — Chinese Acad. of Sci.
Li, Hucheng — Acad. of Mathematics & Sys. Sci., CAS
Zhou, Ye — Chinese Acad. of Sci.
Yang, Xiaoguang — Acad. of Mathematics & Sys. Sci., Chinese Acad. of Sci.

▷ PTuB-76

0848 *Spatial Dynamics of the Public Goods Game with Probabilistic Participation*

Wang, Xiaofeng — DongHua Univ.
Kong, Weijian — Donghua Univ.

▷ PTuB-77

1049 *Discrete Opinion Dynamics with Social Bots on Signed Network*

Luo, Yun — Westlake Univ.
Cheng, Chun — Westlake Univ.
Yu, Changbin — Westlake Univ.

▷ PTuB-78

0053 *The MPC Attitude Control with Integration for VELOX-II*

Zhang, Xiaohua — Nanjing Univ. of Sci. & Tech.
Ling, Keck Voon — Nanyang Technological Univ.
Lim, Wee Seng — Nanyang Technological Univ.
Chong, Kwang Tong — Nanyang Technological Univ.
Lu, Zhengliang — Nanjing Univ. of Sci. & Tech.
Zhang, Xiang — Nanjing Univ. of Sci. & Tech.
Liao, Wenhe — Nanjing Univ. of Sci. & Tech.

▷ PTuB-79

0363 *Adaptive Terminal Sliding Mode Control for the Combined Spacecraft Takeover Control*

Zhou, Heng — National Univ. of Defense Tech.
Zhao, Yong — National Univ. of Defense Tech.
Chen, Zhijun — National Univ. of Defense Tech.

▷ PTuB-80

0365 *Real-Time Simulation Platform Verification for RLV Attitude Control*

Li, Kang — Tianjin Univ.
Zong, Qun — Tianjin Univ.
Zhang, Ruilong — Tianjin Univ.
Zhang, Xiuyun — Tianjin Univ.

▷ PTuB-81

0388 *Cascade Control of Spacecraft Formation with Actuator Saturation*

Cui, Shihang — China Acad. of Space Tech.
Li, Yong — China Acad. of Space Thecnology

▷ PTuB-82

0645 *Trajectory Generation for Quadrotor While Tracking A Moving Target in Cluttered Environment*

Xi, Lele — Beijing Inst. of Tech.
Peng, Zhihong — Beijing Inst. of Tech.
Jiao, Lei — Beijing Inst. of Tech.

▷ PTuB-83

0714 *Observer-like Model Reference Adaptive Augmenting Based Fixed-wing UAV Control*

Xiong, Jizhang — Huazhong Univ. of Sci. & Tech.
Yang, Ye — Beijing Aerospace Automatic Control Institution
Cheng, Zhongtao — Huazhong Univ. of Sci. & Tech.
Liu, Lei — Huazhong Univ. of Sci. & Tech.
Wang, Yongji — Department of Control Sci. & Engineering,Huazhong Univ. of Sci. & Tech.
Fan, Huijin — Huazhong Univ. of Sci. & Tech.

▷ PTuB-84

1011 *Obstacle Avoidance-based Control System Design of UAV with Suspended Payload*

Ren, Zhiheng — Tianjin Univ.
Hu, Chaofang — Tianjin Univ.
Wu, Hao — Tianjin Univ.
Sun, Bing Han — Tianjin Univ.
Guo, Yao — Tianjin Univ.

▷ PTuB-85

1021 *Vision-based Autonomous Landing of Unmanned Aerial Vehicle on A Motional Unmanned Surface Vessel*

Xu, Zhecheng — Huazhong Univ. of Sci. & Tech.
Hu, Binbin — Huazhong Univ. of Sci. & Tech.
Liu, Bin — Huazhong Univ. of Sci. and
Wang, Xudong — Huazhong Univ. of Sci. & Tech.
Zhang, Hai-Tao — Huazhong Univ. of Sci. & Tech.

▷ PTuB-86

1147 *Adaptive Tracking Control for Spacecraft Hovering to Noncooperative Target with Trajectory Generator*

Zhang, Kai — Southwest Jiaotong Univ.
Li, Bin — Sichuan Univ.

▷ PTuB-87

1413 *Controller Design of Aero-engines under the Distributed Architecture with Time Delays*

Wang, Xinyue — Dalian Univ. of Tech.
Du, Xian — Dalian Univ. of Tech.
Wang, Xuefang — Dalian Univ. of Tech.
Sun, Xi-Ming — Dalian Univ. of Tech.
Li, Yingshun — Shenyang Univ. of Tech.

▷ PTuB-88

1688 基于可行配置矩阵的航天器推力器配置构型方法

Spacecraft Thruster Configuration Method Based on Feasible Configuration Matrix

Wang, Min — Beijing Inst. of Control Engineering
Xie, Yongchun — Beijing Inst. of Control Engineering

▷ PTuB-89

1753 *Path Planning of Stand-off Jamming Electronic Warfare Aircraft*

Feng, Qi — Northwestern Polytechnical Univ.
Hong, Chunshen — Northwestern Polytechnical Univ.
Gao, Ruizhou — Sci. & Tech. on Electro-optic Control Laboratory

▷ PTuB-90

1906 *Robust Attitude Tracking Control and Disturbance Rejection for Flexible Spacecraft*

Dong, Hanlin — Harbin Inst. of Tech.
Yang, Xuebo — Harbin Inst. of Tech.

▷ PTuB-91

1929 *Wind Disturbance Rejection Control Law Based on AESO for A Hybrid Tail-Sitter UAV*

Wang, Shuyang — Beihang Univ.
Zhang, Jing — Beihang Univ.
Yang, Lingyu — Beihang Univ.

▷ PTuB-92

2108 *FSE-RBFNNs-Based Adaptive Tracking Control of Hypersonic Flight Vehicles with Uncertain Periodic Time-Varying Disturbances*

Dong, Zehong — Air Force Engineering Univ.
Li, Yinghui — Air Force Engineering Univ.
Zuo, Renwei — Air Force Engineering Univ.
Xu, Haojun — Aeronautics Engineering College
Lv, Maolong — Delft Univ. of Tech.

▷ PTuB-93

2234 *Data-Driven Learning and Receding Horizon Control for Quadrotors*

Hu, Chen — Hangzhou Dianzi Univ.
Lu, Qiang — Hangzhou Dianzi Univ.
Yin, Ke — Hangzhou Dianzi Univ.

▷ PTuB-94

2292 *Simulation Verification of Flight Control of A Tilt Tri-rotor UAV Using X-plane*

He, Guang — National Univ. of Defense & Tech.,
Yu, Li — National Univ. of Defense Tech.
Jia, Shengde — National Univ. of Defense Tech.
Wang, Xiangke — National Univ. of Defense Tech.

▷ PTuB-95

0067 *Covered Vehicle Detection in Autonomous Driving Based on Faster RCNN*

Fan, Jiaqi — Jilin Univ.
Huo, Tianjiao — Jilin Universuty
Li, Xin — Jilin Univ.
Qu, Ting — Jilin Univ.
Gao, Bingzhao — Jilin Univ.

Proceedings of the 39th Chinese Control Conference
July 27-29, 2020, Shenyang, China

Wind Disturbance Rejection Control Law Based on AESO for a Hybrid Tail-Sitter UAV

Shuyang Wang[1], Jing Zhang[1], Lingyu Yang[1]

1. School of Automation Science and Electrical Engineering, Beihang University, Beijing 100191
E-mail: w747922247@163.com

Abstract: Hybrid tail-sitter unmanned aerial vehicles (UAVs) are sensitive to the wind disturbance in the vertical take-off and landing (VTOL) stage, which can easily affect control performance and even stability. Aiming at this problem, this paper proposes a wind disturbance rejection control law based on adaptive extended state observer (AESO). This method combines a nominal control law and a novel disturbance observer. Among them, the nominal control law uses proportional-integral-differential (PID) control method to achieve a good control performance without wind disturbance. The disturbance observer based on AESO algorithm can accurately estimate wind disturbances while eliminating peaking phenomenon under sensor noises. Simulation results demonstrate the effectiveness of the proposed control method.

Key Words: Wind disturbance, Tail-Sitter UAV, adaptive extended state observer, peaking phenomenon.

1 Introduction

The tail-sitter unmanned aerial vehicles (UAVs) have low requirements for take-off and landing locations, and can cruise at high speeds horizontally. In addition, the UAVs have the advantages of good maneuverability, long flight time, and simple structure. Therefore, tail-sitter UAVs are widely used in the military and civilian fields, and have good prospects. In the military field, small tail-sitter UAVs are used for detecting enemy situations, locating and firing, electronic warfare, ground (air) attacks, and communication relays. In the civilian field, tail-sitter UAVs are used in the rescue of natural disasters such as earthquakes and floods, monitoring forest fires, and aerial photography [1].

Hybrid tail-sitter UAVs face problems such as complex low-altitude flight conditions, being sensitive to wind disturbances due to light weight and large windward surface, and severe attitude and position changes after wind disturbance in the vertical take-off and landing (VTOL) stage [2]. It is of great significance to design the wind disturbance rejection control law for the hybrid tail-sitter UAVs in the VTOL stage.

Facing the problem of the wind disturbance, the classic PID control law can no longer meet the control requirements. Wang et al. [3] and Kim et al. [4] used Kalman filtering to estimate aerodynamic parameters online, and measured or estimated wind speed information to compensate for wind effects. This method improves UAV altitude and heading control performance, but it is slower than other methods. Waslander et al. [5] extracted wind speed estimates from accelerometer data to estimate wind disturbances and compensate them. This method can improve accuracy, but the precondition is to attribute all deviations from acceleration to wind disturbances. Xiao et al. [6] repeatedly modified and optimized the rules of the fuzzy controller through improved genetic algorithms and feedback data of the attitude changes, so that the controller had the ability to learn independently. This method can improve the performance of the controller when dealing with wind disturbance. But it is too computationally intensive, and easy to fall into a local optimal solution. It lacks feasibility in the actual vertical take-off and landing stage. and easily falls into a local optimal solution. Qi et al. [7] established a closed-loop control loop for second-order linear active disturbance rejection control (LADRC) and designed a feedback control law to meet requirements of attitude control. The system is robust and has fewer adjustable parameters, which is easy to implement. However, the method has limitations of general linear control methods. In order to realize the stable flight of UAV in wind shear, Xu et al. [8] combined the anti-step adaptive control algorithm with sliding mode control method to obtain the anti-step sliding mode adaptive control algorithm. Simulations show that under the influence of wind shear, the backstep sliding mode adaptive control algorithm is more robust, but its attitude control time is longer than other methods.

In the above literature, there are mainly two methods for dealing with wind disturbance. One method is to directly measure the wind speed or use other known quantities to estimate the wind speed for compensation [3,4,5]. However, it is far less intuitive to estimate the impact of wind on UAV attitude through wind speed changes than to directly measure UAV attitude information. Another method is to directly or linearly control the controlled object based on the attitude error [6,7,8]. However, in these methods, it is generally assumed that the wind speed changes slowly. And they have the disadvantages of complicated structural, slow convergence speed, and excessive calculation. In order to overcome the shortcomings of the above methods, this paper proposes a wind disturbance rejection control law based on adaptive extended state observer (AESO). Proportional -integral-differential (PID) control method is used to stabilize the inner loop without wind disturbance, and the AESO algorithm is used to estimate and compensate for the wind disturbance. This method can directly estimate the disturbance torque to the UAV, and there is no obvious peaking phenomenon under sensor noises.

*This work is supported by National Natural Science Foundation (NNSF) of China under Grant 61273099, 61304030.

2 Hybrid Tail-Sitter UAV Modeling

The hybrid tail-sitter UAV is shown in Fig. 1. This UAV is mainly composed of the fuselage, wings, ailerons, elevators, rudder, fins, propellers and electronics. In the VTOL stage, the propellers provide lift. The UAV attitude control is realized though changes in the speed difference between the left propeller and right propeller, the common inclination of the left and right propellers, and the deflection angle of the two fins [9].

Above all, establish a mathematical model of the UAV in the VTOL stage. For convenience, making the following assumptions when modeling the UAV:

(1) The UAV is a rigid body;

(2) Mass and moment of inertia are time-invariant;

(3) The center of gravity of the UAV is consistent with the geometric center.

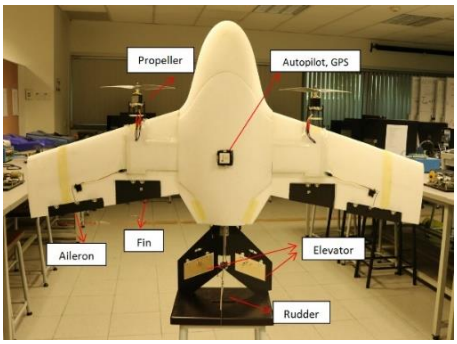

Fig. 1: The hybrid tail-sitter UAV

2.1 Coordinate Frames

In order to solve the singularity problem of Euler angles, the following coordinate frames are established [10]:

- The global inertial frame x, y, z

Select a point O on the ground as the origin of the global inertial frame. Then select a direction through the O point in the horizontal plane as the x-axis direction. The z-axis passes through point O, is perpendicular to the horizontal plane, and points to the center of the earth. The y-axis is in the horizontal plane and is perpendicular to the x-axis and the z-axis. The direction of the y-axis is determined according to the right-hand rule.

- The body frame x_b, y_b, z_b

The center of mass of the UAV is the origin of the body frame. The y_b axis points to the wing tip of the UAV and z_b axis points to the tail of the UAV. The direction of the x_b axis is determined by the right-hand rule.

- The rotor frames x_{ri}, y_{ri}, z_{ri}

The center of each propeller is the origin O_i of each rotor frame. The x_{ri} and y_{ri} axes are on the corresponding propeller plan. The z_{ri} axis passes O_i, and points to the opposite direction of the propeller thrust. The x_{ri}, y_{ri} and z_{ri} axes conform to the right-hand rule. When the propeller is not tilted, the axes of the rotor frames are parallel to the axes of the body frame.

2.2 Kinematic Equations

The conversion relationship between Euler angle and angular velocity is:

$$\begin{pmatrix} \dot{\phi} \\ \dot{\theta} \\ \dot{\psi} \end{pmatrix} = \begin{pmatrix} 1 & \sin\phi\tan\theta & \cos\phi\tan\theta \\ 0 & \cos\phi & -\sin\phi \\ 0 & \dfrac{\sin\phi}{\cos\theta} & \dfrac{\cos\phi}{\cos\theta} \end{pmatrix} \begin{pmatrix} p \\ q \\ r \end{pmatrix} \tag{1}$$

Among them, p, q and r are the UAV's roll angular velocity, pitch angular velocity, and yaw angular velocity; ϕ, θ and ψ are the UAV's roll, pitch, and yaw angles, respectively.

The attitude of the UAV is expressed in the form of a rotation matrix as follows:

$$\dot{\boldsymbol{R}}_{BE} = \boldsymbol{R}_{BE} \begin{pmatrix} 0 & -r & q \\ r & 0 & -p \\ -q & p & 0 \end{pmatrix} \tag{2}$$

$\boldsymbol{R}_{BE}$ is the transformation matrix between the body frame and the global inertial frame.

To avoid singularity problems, a quaternion modeling method is used [11]. The differentiated quaternion matrix is as follows:

$$\begin{pmatrix} \dot{q}_0 \\ \dot{q}_1 \\ \dot{q}_2 \\ \dot{q}_3 \end{pmatrix} = -\frac{1}{2} \begin{pmatrix} 0 & p & q & r \\ -p & 0 & -r & q \\ -q & r & 0 & p \\ -r & -q & p & 0 \end{pmatrix} \begin{pmatrix} q_0 \\ q_1 \\ q_2 \\ q_3 \end{pmatrix} \tag{3}$$

Among them, $q_0 - q_3$ are intermediate quantities for modeling.

2.3 Force Equations

$$\begin{pmatrix} \ddot{x} \\ \ddot{y} \\ \ddot{z} \end{pmatrix} = \begin{pmatrix} 0 \\ 0 \\ g \end{pmatrix} + \frac{1}{m} \boldsymbol{R}_{BE} \boldsymbol{R}_{RB} \begin{pmatrix} 0 \\ 0 \\ -T \end{pmatrix} + \frac{1}{m} \boldsymbol{F}_{surface} + \frac{1}{m} \boldsymbol{F}_{aero} \tag{4}$$

Among them, x, y, z are the position coordinates of the UAV, g is the acceleration of gravity, $\boldsymbol{F}_{surface}$ is the force generated by the deflection of the UAV control surface, $\boldsymbol{F}_{aero}$ is the aerodynamic force received by the UAV, and $\boldsymbol{R}_{RB}$ is the transformation matrix between the rotor frame and the body frame.

Assuming that the inclination and direction of the two propellers are the same in the VTOL stage, the matrix $\boldsymbol{R}_{RB}$ can be written as follows:

$$\boldsymbol{R}_{RB} = \begin{pmatrix} \cos\delta_p & 0 & \sin\delta_p \\ 0 & 1 & 0 \\ -\sin\delta_p & 0 & \cos\delta_p \end{pmatrix} \tag{5}$$

δ_p is the inclination of the propeller.

2.4 Moment Equations

Ignoring the gyro torque of the two propellers, the moment equation of the UAV is simplified into the following form in the body frame:

$$\boldsymbol{I}_f \dot{\boldsymbol{\Omega}}_b = -\boldsymbol{\Omega}_b \times \left(\boldsymbol{I}_f \boldsymbol{\Omega}_b \right) + \boldsymbol{M}_{fin} + \boldsymbol{M}_{prop} + \boldsymbol{M}_{vectorT} \tag{6}$$

Among them, $\boldsymbol{I}_f$ is the moment of inertia matrix, $\boldsymbol{\Omega}_b$ is the vector of angular velocity in the body frame, $\boldsymbol{M}_{fin}$ is the torque vector generated by fin deflection, $\boldsymbol{M}_{prop}$ is the torque vector generated by the speed difference between the left and right propellers, and $\boldsymbol{M}_{vectorT}$ is the torque vector

generated by the thrust vector after the propeller tilts. The expressions for $\boldsymbol{M}_{fin}$, $\boldsymbol{M}_{prop}$ and $\boldsymbol{M}_{vectorT}$ are as follows:

$$\boldsymbol{M}_{fin} = \begin{bmatrix} 0 \\ 0 \\ \frac{1}{2}\rho C_L S l V^2 \end{bmatrix} \tag{7}$$

$$\boldsymbol{M}_{prop} = \boldsymbol{R}_{RB} \begin{bmatrix} 0 \\ 0 \\ M_{prop2} - M_{prop1} \end{bmatrix} \tag{8}$$

$$\boldsymbol{M}_{vectorT} = \boldsymbol{r}_{prop} \times \left[\boldsymbol{R}_{RB} \begin{pmatrix} 0 \\ 0 \\ T \end{pmatrix} \right] \tag{9}$$

In $\boldsymbol{M}_{fin}$, the moments in the pitch direction cancel each other out and can be ignored. ρ is the air density, V is the airspeed, S is the fin reference area, and l is the distance from the center of gravity of the UAV in the y_b direction to the center of the fin. C_L is the yaw control derivative, which can be expressed as: $C_L = 2\pi(\delta_{l1} - \delta_{l2})$, where δ_{l1} and δ_{l2} are the left and right fin deflection angles. $\boldsymbol{M}_{prop1}$, $\boldsymbol{M}_{prop2}$ are the torques generated by the left and right propeller rotations. In $\boldsymbol{M}_{vectorT}$, $\boldsymbol{r}_{prop}$ is the distance vector from the center of gravity of the UAV to the center of the two propellers in the body frame, and T is the force generated by the propeller rotation.

The attitude control of the hybrid tail-sitter UAV is realized by controlling the speed difference between the left and right propellers, the common inclination of the left and right propellers, and the deflection angles of the two fins. The motion state of the UAV can be obtained from the aerodynamic characteristics of the UAV and related dynamic equations.

3 Wind Disturbance Rejection Control Law Based on AESO

The structural framework of wind disturbance rejection control law is shown in Fig. 2:

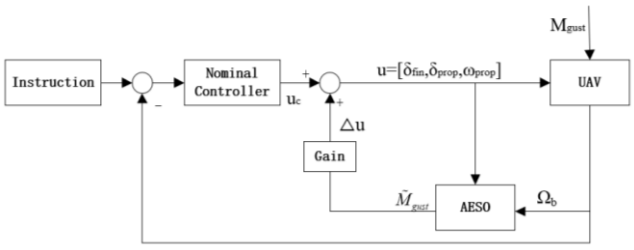

Fig. 2: Wind disturbance rejection control law

For the tail-sitter hybrid UAV, the PID control method is used to control the inner loop's attitude. To solve the problem of wind disturbance in VTOL mode, AESO is used to accurately estimate wind disturbance under sensor noises. In this way, the UAV can stabilize its flight attitude and have good dynamic performance in the VTOL stage under the wind disturbance.

3.1 Nominal Attitude Controller

The PID control method [12-13] is used to control the attitude of the UAV in the VTOL stage. The ultimate goal is to make the UAV fly smoothly under ideal conditions (without wind disturbance).

The influence of the coupling effect between channels can be ignored, and only Euler angle is used as the feedback amount. PID control law for UAV roll, pitch, and yaw channels are designed as follows:

$$\boldsymbol{u}(t) = k_p \boldsymbol{e}(t) + k_d \frac{d\boldsymbol{e}(t)}{dt} + k_i \int_0^t \boldsymbol{e}(t)dt \tag{10}$$

Where k_p is the proportional gain, k_i is the integration time constant, and k_d is the differential time constant. The three channel error expressions are as follows:

Roll channel error: $e_{roll}(t) = \phi - \phi_{ref}$;

Pitch channel error: $e_{pitch}(t) = \theta - \theta_{ref}$;

Yaw channel error: $e_{yaw}(t) = \psi - \psi_{ref}$;

Among them, ϕ, θ and ψ are the actual roll angle, pitch angle, and yaw angle of the UAV, and ϕ_{ref}, θ_{ref} and ψ_{ref} are the expected roll angle, pitch angle, and yaw angle.

3.2 Disturbance Observer

After adding the wind disturbance to the model, the accuracy of the nominal control law will be affected directly. The PID control method can no longer achieve the required control performance. A better control method is needed to achieve the required control goal. A novel disturbance observer is introduced here to estimate and compensate for wind disturbance.

The Extended State Observer (ESO) [14-16] expands the unknown disturbance into a new state variable to estimate the system disturbance and compensate it without any direct information about the disturbance. In ESO, the linear expanded state observer (LESO) has a simple structure and a good function. But when sensor noises are added, the estimations of the LESO change significantly at the initial stage, resulting in peaking phenomenon. However, AESO can eliminate the peaking phenomenon of high-gain LESO to a certain extent while ensuring high estimation accuracy [17]. Therefore, AESO is used to compensate for the wind disturbance.

In order to facilitate the calculation, the moment equation of the UAV is re-formulated as follows:

$$\dot{\boldsymbol{\Omega}}_b = \boldsymbol{F}(\boldsymbol{\Omega}_b) + \boldsymbol{G}(\boldsymbol{\Omega}_b, \boldsymbol{u}) + \Delta\boldsymbol{\Omega}_{gust} \tag{11}$$

Among them:

$$\begin{cases} \boldsymbol{F}(\boldsymbol{\Omega}_b) = \boldsymbol{I}_f^{-1}\left(-\boldsymbol{\Omega}_b \times (\boldsymbol{I}_f \boldsymbol{\Omega}_b)\right) = \boldsymbol{f}(\bullet) \\ \boldsymbol{G}(\boldsymbol{\Omega}_b, \boldsymbol{u}) = \boldsymbol{I}_f^{-1}(\boldsymbol{M}_{fin} + \boldsymbol{M}_{prop} + \boldsymbol{M}_{vectorT}) = \boldsymbol{g}(\bullet) \\ \Delta\boldsymbol{\Omega}_{gust} = \boldsymbol{I}_f^{-1}\boldsymbol{M}_{gust} \end{cases} \tag{12}$$

Among them, $\boldsymbol{u}$ is the reference input. For convenience, $\boldsymbol{F}(\boldsymbol{\Omega}_b), \boldsymbol{G}(\boldsymbol{\Omega}_b, \boldsymbol{u})$ will be abbreviated as $\boldsymbol{f}(\bullet)$, $\boldsymbol{g}(\bullet)$ in the following.

For the nonlinear system (11), the control method based on AESO algorithm is adopted. For the pitch and yaw channels, the AESO for observing $\Delta\boldsymbol{\Omega}_{gust}$ is designed as follows:

Pitch channel:

$$\begin{cases} e_q(t) = z_{q1}(t) - q(t) \\ \dot{z}_{q1}(t) = z_{q2}(t) - l_1(t)e_q(t) + f_q(\bullet) + g_q(\bullet) \\ \dot{z}_{q2}(t) = -l_2(t)e_q(t) \end{cases} \quad (13)$$

Yaw channel:

$$\begin{cases} e_r(t) = z_{r1}(t) - r(t) \\ \dot{z}_{r1}(t) = z_{r2}(t) - l_1(t)e_r(t) + f_r(\bullet) + g_r(\bullet) \\ \dot{z}_{r2}(t) = -l_2(t)e_r(t) \end{cases} \quad (14)$$

Among them, $q(t)$ and $r(t)$ are pitch angular velocity and yaw angular velocity, respectively. z_{q1} is the estimated value of the $\boldsymbol{\Omega}_b$ in the pitch direction; z_{r1} is the estimated value of the $\boldsymbol{\Omega}_b$ in the yaw direction. $e_q(t)$ and $e_r(t)$ are the pitch angular velocity and the yaw angular velocity estimation errors, respectively. z_{q2} is the estimated value of $\Delta\boldsymbol{\Omega}_{gust}$ in the pitch direction; z_{r2} is the estimated value of $\Delta\boldsymbol{\Omega}_{gust}$ in the yaw direction. $l_i(t)$ is the time-varying gain of the observer. Using the AESO convergence theorem proved in [17], $l_i(t)$ is designed as:

$$l_i(\omega(t)) = \frac{(n+1)!}{i!(n+1-i)!}\omega(t)^i, \omega(t) \in R^+ \quad (15)$$

$$\omega(t) = \begin{cases} \omega_1, t \in [0, \mathrm{t}_1) \\ \omega_0(t), t \in [\mathrm{t}_1, \mathrm{t}_2] \\ \omega_2, t \in (\mathrm{t}_2, \infty) \end{cases} \quad (16)$$

Then the formula (17) can be obtained:

$$\lim_{\mathrm{t}\to\infty} |\mathrm{x}_\mathrm{i}(t) - \mathrm{z}_\mathrm{i}(t)| \le \mathrm{o}\left(\left(\frac{1}{\omega_2}\right)^{\mathrm{n+2-i}}\right) \quad (17)$$

Among them, n is the order of AESO, and the order of AESO is 2 for nonlinear system (11). From Equation (17), it can be seen that with the increase of the gain ω_2, the estimation error of AESO will gradually become smaller and approach zero. Therefore, parameter $l_i(t)$ is selected according to the above requirements.

The transition from ω_1 to ω_2 needs to be continuous [17]. A monotonically increasing linear change process is adopted for the hybrid tail-sitter UAV.

For a given form of wind disturbance: $\boldsymbol{M}_{gust} = [0, pitchgust, yawgust]^T$, Observations of wind disturbance is $\tilde{\boldsymbol{M}}_{gust} = \boldsymbol{I}_f \left[0, z_{q2}, z_{r2}\right]^T$.

4 Simulation Results and Analysis

The reference values of the roll channel, pitch channel and yaw channel are set to 0.2 rad. The PID control method's parameter and simulation results of each channel are shown in Fig. 3.

Roll channel: $k_{proll} = 10$, $k_{droll} = 4$;

Pitch channel: $k_{ppitch} = 16$, $k_{dpitch} = 2$;

Yaw channel: $k_{pyaw} = 12.5$, $k_{dyaw} = 2.5$;

The simulation results show that the designed PID control law can achieve a good control performance without wind disturbance.

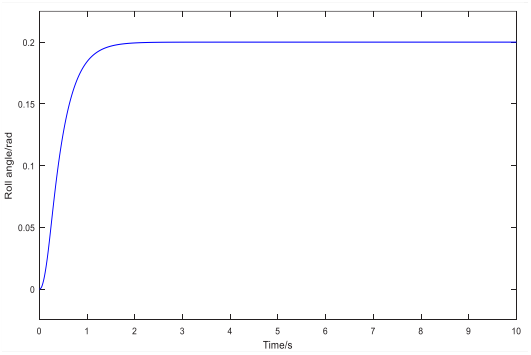

(a) Roll channel

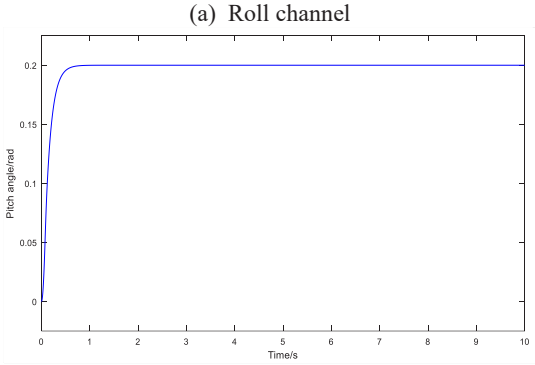

(b) Pitch channel

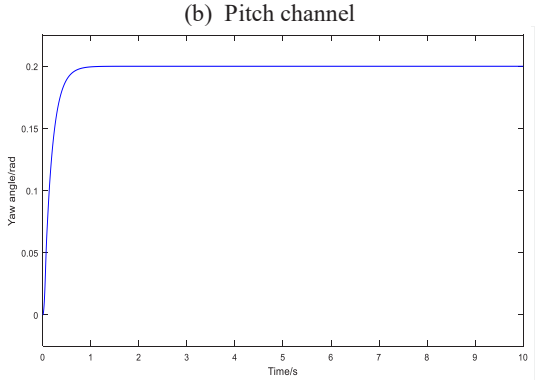

(c) Yaw channel

Fig. 3: Three-channel's attitude angle based on PID control method in an ideal environment

When the pitch and yaw channels are each added a piecewise constant wind disturbance with the maximum amplitude of 1 Nm, the required control performance cannot be achieved by the PID control method alone. At this time, use AESO to estimate and compensate for the disturbance. The comparison between PID control method and the whole wind disturbance rejection control method after adding wind disturbance is shown in Fig. 4.

By comparing the effect of PID-only control method, it can be seen that when AESO is added, AESO compensates for the wind disturbance. Although it cannot completely eliminate the effect of wind disturbance, because it takes time for AESO's error to converge to zero, it can be clearly seen that adding AESO greatly reduce the impact of wind disturbance on the attitude control of the entire system.

The change of the propeller inclination and the fin deflection angle is shown in Fig. 5:

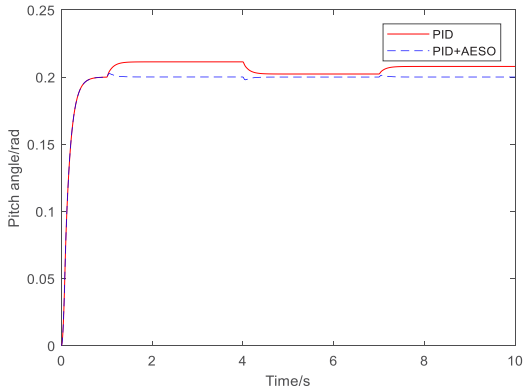

(a) Pitch channel

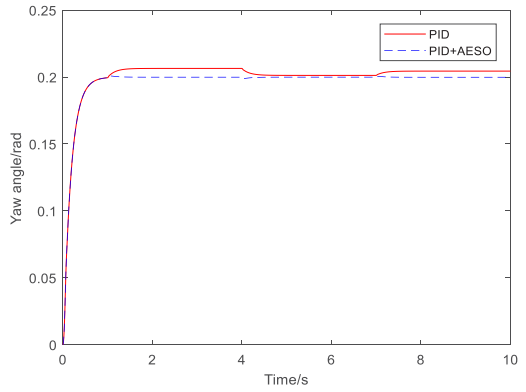

(b) Yaw channel

Fig. 4: Comparisons of the control performance in two channels after adding wind disturbance

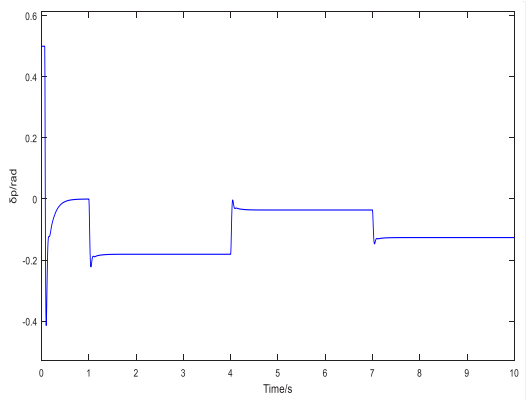

(a) Propeller inclination

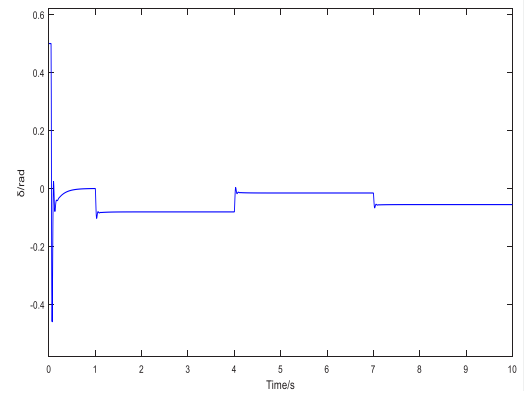

(b) Left fin deflection angle (The right fin deflection angle is opposite to the left one)

Fig. 5: Propeller inclination and fin deflection angle

It can be known from Fig. 5 that the change of the propeller inclination and the fin deflection angle is within a range of ± 0.5 rad, and the actual physical devices can meet this requirement without damaging the control target.

The comparison between wind disturbance and AESO estimates is shown in Fig. 6:

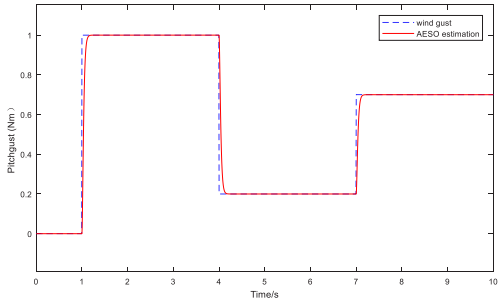

(a) Pitch channel

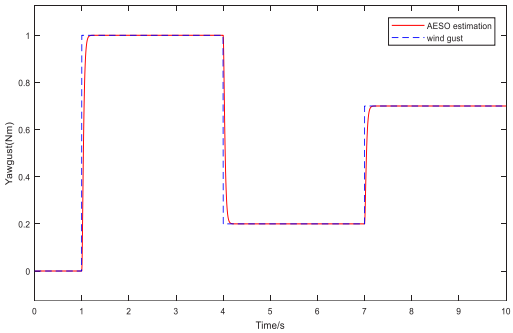

(b) Yaw channel

Fig. 6: Comparisons between the wind disturbance and AESO estimates in two channels

It can be seen from Fig. 6 that the estimations of AESO are basically consistent with the actual wind disturbance. And the unknown wind disturbance is estimated well.

Based on the addition of wind disturbance, random noise signal with a range of ± 5% is added. LESO causes peaking phenomenon due to high gain, and AESO solved this problem. The comparisons between LESO estimations and AESO estimations after adding wind disturbance and sensor noises is shown in Fig. 7, and the statistical data for the first 0.25 seconds is shown in Table 1.

From the simulation results in Fig. 7 and the data in Table 1, it can be seen that the AESO tracks wind disturbance changes rapidly and estimates accurately. After adding sensor noises, it is found that AESO almost completely eliminate the obvious peaking phenomenon of LESO, and the design of AESO achieved good results.

Table 1. Mean squared error of the estimations in the first 0.25s

	Pitch Channel		Yaw Channel	
	LESO	AESO	LESO	AESO
Mean Squared Error (Nm)	0.01819	0.003942	0.02087	0.004889

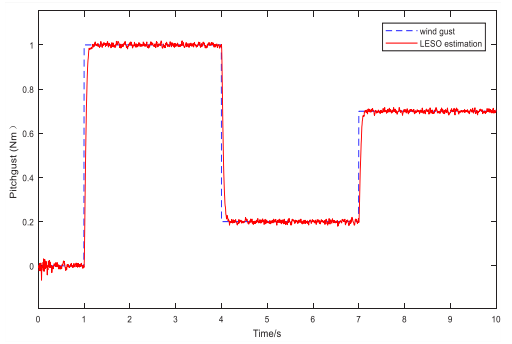

(a) Pitch channel with LESO

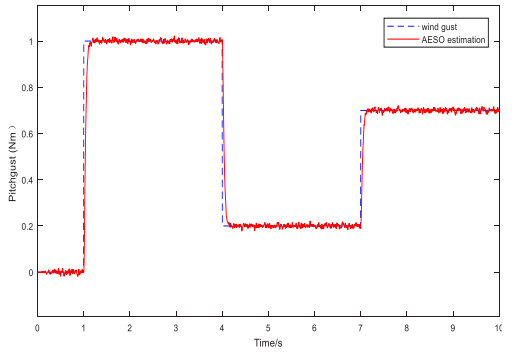

(b) Pitch channel with AESO

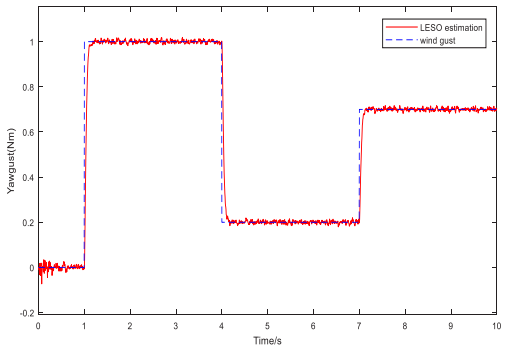

(c) Yaw channel with LESO

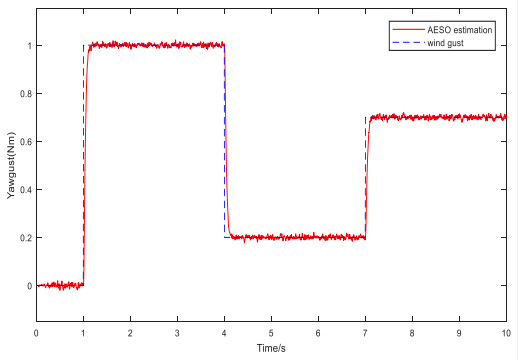

(d) Yaw channel with AESO

Fig. 7: Comparison between LESO estimations and AESO estimations in two channels after adding wind disturbance and sensor noises

5 Conclusion

In this paper, a wind disturbance rejection control law based on AESO is proposed for solving the problem that the hybrid tail-sitter UAV is sensitive to the wind disturbance in the VTOL stage. This method is based on the hybrid tail-sitter UAV model. By designing the nominal control law and the novel disturbance observer, the hybrid tail-sitter UAV attitude control performance is improved in VTOL mode under wind disturbance and sensor noises. The simulation results show that the method has a good effect under wind disturbance, and it can also solve the peaking phenomenon caused by high gain under sensor noises.

References

[1] Y. Liu, *DESIGN OF FLIGHT CONTROLLER FOR A TAIL-SITTER UAV*, Unpublished M.D. dissertation, Harbin Institute of Technology, 2014.

[2] G. Wang, *Research on Position Control Technology of the Unmanned Helicopter in Hover and Low Speed State with Atmospheric Disturbance*, Unpublished M.D. dissertation, Nanjing University of Aeronautics and Astronautics.2013

[3] Z. Wang, Y. Chen, X. Zheng, et al, Quadrotor UAV Control with Disturbance Based on Aerodynamic Parameter Estimation, *Information and Control*, 2018, 47(06):27-34.

[4] M. Kim, Y. Kim, Error Dynamics-Based Guidance Law of UAVs for Target Observation under Wind disturbance, *Infotech*. 2006.

[5] S. Waslander, C. Wang, Wind Disturbance Estimation and Rejection for Quadrotor Position Control, *Aiaa Infotech @aerospace Conference & Aiaa Unmannedunlimited Conference*, 2009.

[6] C. Xiao, Y. Mao, H. Yuan, et al, Design and Simulation of Intelligent Control Algorithm for Quad-rotors under Wind Disturbance, *Computer Science*, 2018, v.45(05):317-323.

[7] H. Qi, X. Qi, Research on quadrotor UAV based on linear active disturbance rejection control technique under wind-disturbance, *Flight Dynamics*, 2018, v.45(05):317-323.

[8] J Xu, Design of BSSA Controller for Unmanned Aerial Vehicle Disturbing to Wind Shear, *Journal of Sichuan University of Science & Engineering (Natural Science Edition)*, 2017(6): 47-53

[9] Y Ke, K Wang, B Chen, Design and Implementation of a Hybrid UAV with Model-Based Flight Capabilities. *IEEE/ASME Transactions on Mechatronics*, 2018:1-1.

[10] S Wu, *Flight Control System*, Beihang University Press, 2013.

[11] X Jing, X. Pan, Quadrotor aircraft attitude control based on quaternion, *Modern Electronics Technique*, 2018, v.41；No.519(16):124-127.

[12] Q Jin, Z Deng, PID Control Principle and Techniques of Parameter Tuning, *Journal of Chongqing Institute of Technology*, 2008.

[13] L Liu, *Research and Application on the PID Parameters Tuning Technology*, Unpublished M.D. dissertation, Zhengzhou University, 2010.

[14] J Han, Nonlinear State Error Feedback Control Law-NLSEF, *Control and Decision*,1995(3):221-225.

[15] J Han, Auto-disturbances-rejection Controller and Its Applications, *Control and Decision*.1998(1):19-23.

[16] J Han, R Zhang, ERROR ANALYSIS OF THE SECOND ORDER ESO, *J. Sys. Sci.& Math. Scis*, 1999(4):465-471.

[17] Z Chen, Q Gao, Convergence analysis and application of adaptive extended state observer, *Control Theory & Applications*, 2018, 35(11): 1697 – 1702.